

РАДІОСПЕКТРОСКОПІЯ

RADIO SPECTROSCOPY

DOI: <https://doi.org/10.15407/rpra30.02.141>

UDC 539.1

PACS numbers: 33.20.-t, 95.30.Ky

E.A. Alekseev^{1,2}, O.I. Baskakov³, S.P. Dyubko^{2,3}

¹ Université de Lille, CNRS, UMR 8523, PhLAM - Physique des Lasers
Atomes et Molécules F-59000 Lille, France

² Institute of Radio Astronomy of the NAS of Ukraine
4, Mystetstv St., Kharkiv, 61002, Ukraine

³ V.N. Karazin Kharkiv National University
4, Svoboda Sq., Kharkiv, 61022, Ukraine
E-mail: yevgeniy.alyekseyev@univ-lille.fr; ealekseev@rian.kharkov.ua

MILLIMETER AND SUB-MILLIMETER-WAVE SPECTRUM OF SELENIUM DIOXIDE, SeO_2

Subject and Purpose. The work is aimed at investigating the spectra of the ground-state and a few of the excited vibrational states for the main isotopologues of the selenium dioxide molecule, SeO_2 , in order to provide a reliable basis for its further search in the interstellar medium.

Method and methodology. The method is based on real-life measurements and onward analysis of the microwave rotational spectrum of the SeO_2 molecule. The measurements are carried out with an automated millimeter wave spectrometer of the Institute of Radio Astronomy of the NAS of Ukraine, (Kharkiv, Ukraine), and the submillimeter-wave spectrometer of the V.N. Karazin Kharkiv National University (Kharkiv, Ukraine).

Results. The measurements were carried out within a range between 70GHz and 500 GHz, where frequencies of about 650 rotational transitions were measured. Most of these belong to the $^{76}\text{SeO}_2$, $^{77}\text{SeO}_2$, $^{78}\text{SeO}_2$, $^{80}\text{SeO}_2$, and $^{82}\text{SeO}_2$ molecules in their respective vibrational ground states. The rest of the lines can be assigned to isotopic species of the $^{76}\text{SeO}_2$, $^{77}\text{SeO}_2$, $^{78}\text{SeO}_2$, $^{80}\text{SeO}_2$, and $^{82}\text{SeO}_2$ molecules in their excited vibrational state $v_2 = 1$, while in the case of $^{80}\text{SeO}_2$ in the excited state $v_2 = 2$ as well. In addition, tentative assignments have been suggested for 10 transitions in the ground-state isotopic species of $^{74}\text{SeO}_2$.

Conclusions. The transitions between states characterized by quantum numbers J up to 70 and quantum numbers K_a up to 19, embracing the ground-state and first-, and second-order excited vibrational states of the $^{74}\text{SeO}_2$, $^{76}\text{SeO}_2$, $^{77}\text{SeO}_2$, $^{78}\text{SeO}_2$, $^{80}\text{SeO}_2$, and $^{82}\text{SeO}_2$ molecules have been identified. Based on these assigned transitions, significantly improved estimates have been obtained for sets of rotational and centrifugal distortion constants, including octic ones, as well as for A-reduced Watson's Hamiltonian in the I' coordinate representation. The parameter sets obtained provide for reliable predictions for possible future astronomical search of the most abundant isotopic species of the SeO_2 molecule.

Key words: selenium dioxide molecule, millimeter wave spectrum, asymmetric top, isotopic substitution.

Introduction

The bent triatomic molecules have, for quite a long time, been an object of extensive spectroscopic studies within the microwave and infrared range. For exam-

ple, the spectrum of the water vapor molecule H_2O has been under investigation up till now [1–4]. The molecule happens to be detected even in stellar and planetary atmospheres [5–7]. Other well-known examples of a bent triatomic molecule are the ozone,

Citation: Alekseev, E.A., Baskakov, O.I., Dyubko, S.P., 2025. Millimeter and sub-millimeter-wave spectrum of selenium dioxide, SeO_2 . *Radio Phys. Radio Astron.*, **30**(2), pp. 141–158. <https://doi.org/10.15407/rpra30.02.141>

© Publisher PH "Akademperiodyka" of the NAS of Ukraine, 2025

 This is an Open Access article under the CC BY-NC-ND 4.0 license (<https://creativecommons.org/licenses/by-nc-nd/4.0/legalcode.en>)

O_3 , and sulfur dioxide SO_2 . Ozone plays an important role within the Earth's atmosphere, so the spectrum of the O_3 molecule has been studied quite well [8, 9]. The sulfur dioxide SO_2 molecule is a well-known atmospheric pollutant, while it is considered to be a secondary frequency standard, applied rather widely for investigating other molecules [10]. That is the reason why its spectrum is being thoroughly studied. A rich volume of data is available on the SO_2 molecule and its isotopic species, both in their ground state and some of the excited vibrational states [11–17]. Note the molecule to have recently been detected in exoplanetary atmospheres [18, 19].

The selenium dioxide, SeO_2 , is a bent triatomic molecule quite similar to the SO_2 . The SeO_2 molecule is of great interest since it has a rather large number of isotopic species corresponding to stable selenium isotopes. The abundance of selenium isotopes is sufficient for allowing rotational spectrum observations with the use of samples with a natural concentration of isotopes. Due to such properties, the rotational spectrum of this molecule is of great importance for the study of the effect of isotopic substitution upon spectroscopic parameters. Because of its toxicity, the molecule may also be considered a pollutant [20].

Also, the interest toward the molecule of selenium dioxide stems from the possibility of its detection in the interstellar medium (ISM) through observations of field radiation from or absorption within it, both owing to rotational transitions. Note that a number of sulfur-containing molecules, like SO and SO_2 , have already been detected in the ISM [21, 22] through observation of their emission lines with rather good signal-to-noise ratios. Note the natural abundances of the isotopes ^{32}S and ^{34}S to be 94.93 and 4.29% respectively, so at least one line of the ^{34}SO molecule could have been detected. According to [23–25], the natural level of titanium abundance in the Universe is more than two orders of magnitude lower than such of sulfur. Nevertheless, some titanium-containing molecules (specifically, TiO and TiO_2) have recently been detected in the ISM [26]. Among these molecules, the titanium dioxide TiO_2 is a bent triatomic one. It is also quite similar to the molecule of selenium dioxide. Again, according to [23–25], the natural level of selenium abundance in the Universe is about two orders of magnitude lower than such of titanium. Nevertheless, taking into account the considerable progress in the development

of experimental equipment and techniques we can expect detection of selenium-containing molecules to happen rather soon. These are the reasons why reliable spectroscopic data on the molecule SeO_2 will be necessary.

In contrast to the molecule SO_2 , the currently available microwave data on the SeO_2 are quite limited. The rotational microwave spectrum thereof was studied somewhat earlier by Takeo et al. [27, 28]. They measured about 90 rotational transitions between 8 and 36 GHz that belonged to the ground- and certain excited vibrational states of the most abundant isotopic species, specifically $^{76}SeO_2$ (9.02%), $^{77}SeO_2$ (7.58%), $^{78}SeO_2$ (23.52%), $^{80}SeO_2$ (49.82%), and $^{82}SeO_2$ (9.19%) [27]. (Here, the figures in the parentheses are relative abundances of the isotopologues represented). The accuracy of their measurements was about ± 0.3 MHz. The rotational constants for the isotopic species staying in the vibrational states under investigation were derived from experimental data. In view of the rather limited amount of these data the quartic centrifugal distortion constants were obtained exclusively from the experimental spectrum for the ground state of the $^{80}SeO_2$ as the most abundant species. The constants for the $^{78}SeO_2$ were calculated from such for the $^{80}SeO_2$. The equilibrium structure of selenium dioxide and its force field were estimated as well.

Then we presented a detailed study of the $^{80}SeO_2$ in its vibrational ground state [29]. The rotational and the centrifugal distortion constants were determined, up to octic ones. Also we published a series of preliminary results for the most widespread isotopic species of SeO_2 (specifically, $^{76}SeO_2$, $^{77}SeO_2$, $^{78}SeO_2$, $^{80}SeO_2$, and $^{82}SeO_2$) in their ground states and some of the excited vibrational states [30]. It should be pointed out that the SeO_2 was also investigated well beyond the microwave range. For example, the authors of paper [29] presented an analysis of the 419-nm absorption system. Similarly, the spectrum of the 313-nm band system of SeO_2 has recently been given a detailed study [32, 33].

Within this work we performed an exploration of the millimeter- and submillimeter wavelength spectrum of SeO_2 . The present investigation has shown that our previous analysis now requires a good deal of improvement. So, the current article may be considered as a continuation of our preceding work [29, 30].

1. Details of experiment

Our investigations were started as measurements of the SeO_2 spectrum, with the use of the submillimeter-wavelength spectrometer that previously belonged to the V.N. Karazin Kharkiv National University (Kharkiv, Ukraine) [34]. The radiation source of the spectrometer was implemented as a submillimeter-wavelength backward wave oscillator (BWO). The output radiation from the BWO was parametrically stabilized in frequency. Transition frequencies were measured with a custom-made wavemeter with a commercial frequency counter back-end. The spectrometer was able to cover the (prescribed) frequency range between 330 and 500 GHz by means of employing a shift BWO. The estimated error level of frequency determination with the spectrometer was about ± 20 kHz. However, for some of the spectral lines the errors could exceed ± 50 kHz as most of the SeO_2 transitions were measured with rather poor signal-to-noise ratios.

Much later a number of more accurate millimeter-wave measurements were performed with a recently designed and constructed millimeter-wave spectrometer [35, 36] based on a computer-controlled millimeter-wave frequency synthesizer. Currently the spectrometer covers the frequency range of 34...420 GHz. It should be noted that measurements for the SeO_2 molecule were started from 70 GHz because of attenuation in the high-temperature absorbing cell (see below). The accuracy of frequency determination for this spectrometer is estimated as ± 1 kHz. However, because of the poor signal-to-noise ratio during measurements of SeO_2 transitions, this level of accuracy could not be achieved. Still, the estimate we have for the conditions of the experiments being discussed is not worse than ± 10 kHz.

Since the optimum vapor pressure for the SeO_2 sample corresponds to temperatures about 150 °C [27], special high-temperature absorbing cells were constructed. We applied two different absorbing cells, intended for measurements within millimeter and submillimeter wavelength ranges, respectively. The submillimeter-wave cell was a 2 meters long, hollow quasi-optical waveguide made of quartz and subject to heating by a nichrome-wire heater that sat on the external surface of the waveguide. The millimeter-wave absorbing cell was a stainless steel waveguide, heated by the electric current from a special

power supply. As had been found, that cell introduced relatively high attenuation at frequencies below 70 GHz, prompting one to consider that value as the low frequency limit to the range of spectral measurements for the SeO_2 molecule.

During the measurements we faced some difficulties, similar to those described by Takeo et al. [27]. The selenium dioxide vapor kept condensing at the colder parts of the cells and decomposing on surfaces of the hotter ones. It was necessary to open the cells from time to time and to clean them thoroughly. Unlike Takeo et al. [27], we did not apply Stark's modulation, accordingly never faced problems stemming from the base line drift.

2. Results and analysis

The selenium dioxide represents a prolate, asymmetric-top molecule possessing an electric dipole moment $\mu_b = 2.62 \pm 0.05$ D and capable of participating in *b*-type transitions [27]. A feature of this molecule is the presence of relatively low-lying excited vibrational states, $\nu_2 = 1$ at 372.5 cm⁻¹ [28] and $\nu_2 = 2$ at about 745 cm⁻¹. This means that at an experimental temperature of +150 °C a number of transitions might be observable between the lines that belong to the above mentioned states. As a result, about 650 transitions of different isotopic species of the SeO_2 molecule, both in the ground- and some of the excited states, were measured within the frequency range between 70 and 500 GHz. Still, the energies of the states $\nu_2 = 1$ and $\nu_2 = 2$ are high enough for independently performing analyses of the rotational spectra for the ground- and excited states.

2.1. Vibrational ground state

The results of measurements for the ground state of SeO_2 are listed in Table 1. Presented in the first column are measured values of the transition frequencies, f_m (MHz). The six following columns contain corresponding quantum numbers J , K_a , K_c of the lower, and J' , K'_a , K'_c of the upper level, respectively. Finally, the differences $f_m - f_c$ (MHz) are listed between the measured, f_m , and the calculated, f_c , frequencies.

The basis for assignment has been derived from rotational constants for the $^{76}\text{SeO}_2$, $^{77}\text{SeO}_2$, $^{78}\text{SeO}_2$, $^{80}\text{SeO}_2$, and $^{82}\text{SeO}_2$ isotopic species, as well as quartic constants of centrifugal distortions for the $^{80}\text{SeO}_2$

Table 1. The ground and excited $\nu_2 = 1$ state transition frequencies (MHz) of SeO_2 molecule

Measured frequency f_m	Lower level			Upper level			Residual $f_m - f_c$	Measured frequency f_m	Lower level			Upper level			Residual $f_m - f_c$
	J	K_a	K_c	J'	K'_a	K'_c			J	K_a	K_c	J'	K'_a	K'_c	
$^{76}\text{SeO}_2$, ground state															
71054.951	16	5	11	17	4	14	-0.007	352958.569	37	6	32	37	5	33	-0.019
330379.651	60	11	49	60	10	50	0.013	353683.740	26	0	26	25	1	25	-0.005
330696.421	68	13	55	68	12	56	-0.006	353902.966	25	2	24	24	1	23	-0.006
330785.409	42	10	32	42	9	33	0.012	354372.958	27	9	19	27	8	20	0.010
332187.561	9	5	5	8	4	4	0.008	354987.487	46	10	36	45	11	35	0.009
332817.935	33	5	29	33	4	30	-0.019	355501.208	17	4	14	16	3	13	-0.020
332859.595	13	4	10	12	3	9	-0.001	355606.865	26	9	17	26	8	18	0.013
335407.315	28	5	23	27	6	22	0.027	357297.995	25	8	18	25	9	17	-0.029
336119.870	56	10	46	56	9	47	-0.014	438058.755	33	11	23	33	10	24	-0.016
336127.120	56	12	44	56	11	45	0.001	460260.818	24	4	20	25	5	21	0.036
336572.955	12	3	9	11	2	10	-0.016	460315.977	34	0	34	33	1	33	-0.046
337003.165	37	9	29	37	8	30	-0.018	460441.735	32	1	31	33	2	32	0.007
337788.054	39	9	31	39	8	32	0.011	460648.987	32	2	30	31	3	29	-0.003
338221.894	32	9	23	32	8	24	-0.004	473638.925	35	1	35	34	0	34	-0.025
338679.284	31	4	28	31	3	29	0.009	473760.064	34	1	33	33	2	32	-0.032
339917.614	42	9	33	41	10	32	-0.029	473826.212	32	3	29	31	4	28	-0.032
340449.210	24	1	23	23	2	22	0.014	474022.465	33	3	31	32	2	30	-0.021
340963.960	12	4	8	11	3	9	-0.050	474522.333	39	12	28	39	11	29	-0.012
341741.084	52	9	43	52	8	44	0.012	479800.310	36	12	24	36	11	25	-0.018
342492.211	41	9	33	41	8	34	0.011	480987.160	32	4	28	31	5	27	0.019
342599.641	33	9	25	33	8	26	0.004	481304.201	35	12	24	35	11	25	0.029
343622.551	34	4	30	34	3	31	-0.005	481796.624	16	6	10	15	5	11	0.017
343626.722	23	3	21	22	2	20	-0.021	482621.449	34	11	23	34	12	22	0.039
343736.935	44	7	37	44	6	38	0.014	484915.893	32	12	20	32	11	21	-0.035
343935.937	41	8	34	41	7	35	0.002	485095.691	44	3	41	44	4	40	-0.049
344796.957	48	8	40	48	7	41	-0.003	490328.154	24	11	13	24	12	12	0.037
345975.282	39	7	33	39	6	34	0.000	491013.958	22	12	10	22	11	11	-0.024
346243.963	30	8	22	30	9	21	-0.015	491286.575	21	12	10	21	11	11	-0.005
346685.439	15	4	12	14	3	11	-0.024	494470.683	17	6	12	16	5	11	0.019
346769.576	31	8	24	31	9	23	-0.037	494925.758	14	7	7	13	6	8	0.041
347602.673	10	5	5	9	4	6	0.021	498856.445	45	4	42	45	5	41	0.039
350819.057	29	9	21	29	8	22	0.008	500280.250	37	1	37	36	0	36	0.025
351856.549	32	3	29	32	2	30	0.020	500396.090	35	2	34	36	1	35	0.056
352469.770	40	10	30	40	9	31	-0.005	500615.121	34	2	32	35	3	33	0.035
352718.281	24	2	22	23	3	21	-0.006	500780.511	34	3	31	33	4	30	0.007
$^{77}\text{SeO}_2$, ground state															
73772.920	40	16	24	39	17	23	-0.009	352475.243	23	4	20	24	3	21	-0.072
331145.258	9	5	5	8	4	4	0.035	353371.547	26	0	26	25	1	25	-0.034
331774.905	13	4	10	12	3	9	0.040	353586.919	25	2	24	24	1	23	-0.013
332978.795	33	5	29	33	4	30	0.000	353612.715	26	9	17	26	8	18	-0.002
334024.460	60	11	49	60	10	50	-0.020	354161.126	17	4	14	16	3	13	0.027

Table 1. Continued

Measured frequency f_m	Lower level			Upper level			Residual $f_m - f_c$	Measured frequency f_m	Lower level			Upper level			Residual $f_m - f_c$
	J	K_a	K_c	J'	K'_a	K'_c			J	K_a	K_c	J'	K'_a	K'_c	
335214.075	37	9	29	37	8	30	-0.003	355337.455	25	9	17	25	8	18	-0.005
335847.855	32	9	23	32	8	24	-0.050	355699.387	30	2	28	30	1	29	0.010
336262.830	39	9	31	39	8	32	0.028	356483.125	24	9	15	24	8	16	-0.004
336453.370	12	3	9	11	2	10	0.046	438502.785	31	10	22	31	11	21	-0.054
337053.660	35	9	27	35	8	28	-0.027	460035.246	33	2	32	32	1	31	0.036
338713.091	31	4	28	31	3	29	0.010	460242.900	32	2	30	31	3	29	-0.001
339869.176	56	10	46	56	9	47	0.020	474777.184	9	7	3	10	8	2	-0.034
340050.430	25	1	25	24	0	24	-0.009	479974.980	34	12	22	34	11	23	0.022
340254.764	12	4	8	11	3	9	0.011	480498.193	16	6	10	15	5	11	0.026
340571.415	33	9	25	33	8	26	0.043	480945.170	32	4	28	31	5	27	-0.031
343210.478	23	3	21	22	2	20	0.014	481205.558	33	11	23	33	12	22	0.036
344252.457	42	9	33	41	10	32	-0.022	484975.875	29	12	18	29	11	19	0.068
345125.508	52	9	43	52	8	44	0.035	493089.758	17	6	12	16	5	11	-0.021
345451.737	15	4	12	14	3	11	0.005	493417.941	14	7	7	13	6	8	-0.034
345568.305	48	11	37	48	10	38	0.017	495345.139	49	12	38	49	13	37	-0.042
346195.005	39	7	33	39	6	34	-0.024	496752.990	48	12	36	48	13	35	0.028
346558.275	10	5	5	9	4	6	-0.011	499839.353	37	1	37	36	0	36	-0.008
347547.082	48	8	40	48	7	41	-0.024	499954.687	36	1	35	35	2	34	0.009
349123.476	40	10	30	40	9	31	-0.028	500171.126	35	3	33	34	2	32	-0.004
349663.707	28	9	19	28	8	20	-0.070	500351.482	34	3	31	33	4	30	0.063
352380.089	27	9	19	27	8	20	-0.007								
$^{78}\text{SeO}_2$, ground state															
71057.926	24	10	14	23	11	13	0.005	439515.235	28	11	17	28	10	18	-0.051
71260.736	32	13	19	31	14	18	-0.002	445723.190	30	3	27	29	4	26	-0.005
72974.113	45	16	30	46	15	31	0.000	446094.982	11	7	5	10	6	4	0.000
73641.054	37	13	25	38	12	26	-0.002	446212.482	33	1	33	32	0	32	-0.005
330132.760	9	5	5	8	4	4	-0.009	446338.382	32	1	31	31	2	30	-0.026
330718.110	12	3	9	13	4	10	-0.032	446664.285	31	3	29	30	2	28	-0.017
333059.280	47	10	38	46	11	35	0.023	449056.783	14	6	8	13	5	9	0.011
333134.375	33	5	29	33	4	30	0.021	459513.745	34	0	34	33	1	33	-0.010
333492.510	37	9	29	37	8	30	-0.011	459638.131	32	1	31	33	2	32	0.046
333527.325	32	9	23	32	8	24	0.019	460749.765	27	5	23	26	4	22	0.002
333564.605	64	12	52	64	11	53	-0.005	460973.620	42	11	31	42	12	30	0.019
334091.745	68	13	55	68	12	56	-0.002	470189.297	48	6	42	48	5	43	-0.043
334805.815	39	9	31	39	8	32	-0.015	470933.354	38	12	26	38	11	27	-0.018
335166.200	35	9	27	35	8	28	-0.006	472654.889	52	13	39	52	12	40	-0.035
336342.760	12	3	9	11	2	10	0.002	472813.602	34	0	34	35	1	35	-0.005
339756.870	25	1	25	24	0	24	0.020	472890.092	37	11	27	37	12	26	0.029
339860.597	24	1	23	23	2	22	0.018	472933.634	34	1	33	33	2	32	0.005
339895.230	28	5	23	27	6	22	-0.027	473066.332	32	3	29	31	4	28	0.008
340218.860	41	9	33	41	8	34	-0.049	473126.976	10	8	2	9	7	3	0.008
340439.045	62	12	50	62	13	49	0.030	474501.087	36	12	24	36	11	25	-0.036

Table 1. Continued

Measured frequency f_m	Lower level			Upper level			Residual $f_m - f_c$	Measured frequency f_m	Lower level			Upper level			Residual $f_m - f_c$
	J	K_a	K_c	J'	K'_a	K'_c			J	K_a	K_c	J'	K'_a	K'_c	
340650.050	40	6	34	40	5	35	0.027	475275.330	41	4	38	41	3	39	0.019
343571.573	56	10	46	56	9	47	0.032	480766.902	31	12	20	31	11	21	0.007
344250.398	15	4	12	14	3	11	-0.004	480886.498	32	4	28	31	5	27	0.011
344270.755	34	4	30	34	3	31	0.049	481665.508	30	12	18	30	11	19	0.013
345543.951	10	5	5	9	4	6	-0.017	482471.198	29	11	19	29	12	18	0.085
345836.956	40	9	31	40	10	30	0.027	483188.437	28	12	16	28	11	17	-0.017
346419.699	39	7	33	39	6	34	0.007	483826.073	27	11	17	27	12	16	0.059
346827.432	29	9	21	29	8	22	0.008	484389.801	26	11	15	26	12	14	0.048
347656.512	28	9	19	28	8	20	-0.003	484886.104	25	12	14	25	11	15	-0.010
347721.026	44	7	37	44	6	38	-0.005	485145.660	44	4	40	44	3	41	0.012
351963.753	32	2	30	32	3	29	-0.042	485320.636	24	11	13	24	12	12	-0.101
352230.303	24	2	22	23	3	21	-0.002	491746.268	17	6	12	16	5	11	0.027
352715.219	24	3	21	23	4	20	0.013	492227.825	49	13	37	49	12	38	-0.006
352858.066	17	4	14	16	3	13	0.009	493329.887	47	6	42	47	5	43	-0.002
353278.340	25	2	24	24	1	23	0.005	493524.031	48	13	35	48	12	36	-0.033
353325.806	53	12	42	52	13	39	-0.003	495132.088	18	4	14	17	3	15	0.014
353432.300	25	9	17	25	8	18	0.002	498354.657	45	10	36	46	9	37	-0.015
353486.109	37	6	32	37	5	33	0.028	498367.799	47	12	36	47	13	35	0.064
354586.863	24	8	16	24	9	15	-0.001	498896.785	36	6	30	35	7	29	0.002
355316.405	68	14	54	68	13	55	-0.014	499296.019	58	14	44	58	13	45	0.017
355591.125	30	1	29	30	2	28	-0.025	499408.796	36	0	36	37	1	37	0.004
355792.264	23	9	15	23	8	16	-0.004	499523.508	36	1	35	35	2	34	-0.022
356520.826	28	1	27	28	0	28	-0.016	499737.503	34	2	32	35	3	33	0.030
357513.245	8	6	2	7	5	3	0.012	499931.103	34	3	31	33	4	30	-0.021
437385.388	30	11	19	30	10	20	-0.021	499982.924	9	9	1	8	8	0	-0.021
437430.758	43	6	38	43	5	39	0.003	500427.443	46	12	34	46	13	33	-0.037
438521.723	29	11	19	29	10	20	-0.028								
$^{80}\text{SeO}_2$, ground state															
73327.192	42	15	27	43	14	30	-0.029	445588.086	31	2	30	32	1	31	-0.021
73440.840	8	0	8	8	1	7	0.031	445901.712	30	2	28	31	3	29	-0.027
73589.960	26	9	17	27	8	20	0.015	446637.465	13	5	9	14	6	8	-0.032
73919.710	16	5	11	17	4	14	-0.013	447545.452	30	4	26	29	5	25	-0.008
74611.185	50	18	32	51	17	35	0.008	447560.492	49	8	42	49	7	43	-0.009
330217.830	37	9	29	37	8	30	-0.003	447585.942	54	13	41	54	12	42	-0.002
330709.270	36	5	31	36	4	32	0.041	447964.446	39	4	36	39	3	37	-0.020
330893.005	62	13	49	62	12	50	-0.001	447973.498	44	11	33	44	12	32	0.007
331550.161	35	9	27	35	8	28	-0.027	447987.635	45	12	34	45	11	35	-0.016
332064.935	39	8	32	39	9	31	0.060	449448.317	21	5	17	20	4	16	0.038
332310.326	48	11	37	48	10	38	0.013	449835.266	37	2	36	37	3	35	0.018
332653.910	49	11	39	48	12	36	-0.018	458742.331	33	1	33	34	0	34	-0.032
332837.005	23	16	8	22	17	5	-0.052	458865.382	32	1	31	33	2	32	-0.008
333036.636	55	10	46	54	11	43	0.037	459073.553	31	3	29	32	2	30	0.052

Table 1. Continued

Measured frequency f_m	Lower level			Upper level			Residual $f_m - f_c$	Measured frequency f_m	Lower level			Upper level			Residual $f_m - f_c$
	J	K_a	K_c	J'	K'_a	K'_c			J	K_a	K_c	J'	K'_a	K'_c	
333153.400	48	11	37	47	12	36	-0.006	459283.664	41	12	30	41	11	31	-0.028
333432.555	33	5	29	33	4	30	0.019	460677.820	30	3	27	31	4	28	0.000
333877.653	59	16	44	60	15	45	0.006	460954.274	14	5	9	15	6	10	-0.032
334452.624	70	14	56	70	13	57	0.016	465780.683	38	11	27	38	12	26	-0.053
334820.575	33	9	25	33	8	26	-0.004	465845.727	45	5	41	45	6	40	-0.041
336070.170	28	18	10	27	19	9	0.040	467806.655	37	11	27	37	12	26	-0.010
336145.250	12	3	9	11	2	10	-0.026	468091.069	28	4	24	29	5	25	-0.014
336173.455	47	10	38	46	11	35	-0.021	469453.528	36	12	24	36	11	25	-0.008
337017.934	62	17	45	63	16	48	-0.040	469942.807	9	7	3	10	8	2	-0.009
337823.620	30	9	21	30	8	22	-0.009	471050.469	35	12	24	35	11	25	-0.013
338178.685	41	9	33	41	8	34	0.011	471078.273	48	6	42	48	5	43	0.035
338252.945	12	4	8	11	3	9	-0.005	471525.424	43	5	39	43	4	40	0.011
338664.579	20	15	5	19	16	4	-0.067	472019.974	34	0	34	35	1	35	-0.034
338795.687	31	4	28	31	3	29	0.016	472060.849	54	8	46	54	7	47	0.027
338915.260	31	9	23	31	8	24	0.003	472138.972	34	1	33	33	2	32	0.025
339185.645	25	1	25	24	0	24	-0.005	472327.510	31	4	28	32	3	29	-0.032
339293.976	24	1	23	23	2	22	-0.011	472386.360	33	3	31	32	2	30	-0.003
339392.265	40	10	30	40	9	31	0.025	472435.300	34	12	22	34	11	23	-0.031
339796.622	6	5	1	7	6	2	0.016	472686.268	53	12	42	53	13	41	-0.063
340235.275	64	11	53	64	12	52	-0.026	473717.333	33	11	23	33	12	22	-0.078
340856.580	38	8	30	37	9	29	-0.028	474855.793	32	12	20	32	11	21	-0.039
342667.481	27	2	26	27	1	27	-0.006	475053.463	41	4	38	41	3	39	-0.006
343113.393	40	6	34	40	5	35	-0.011	475888.237	31	12	20	31	11	21	-0.009
343586.767	10	5	5	9	4	6	-0.003	480114.157	25	12	14	25	11	15	0.000
344845.854	55	13	43	54	14	40	-0.025	480560.274	24	12	12	24	11	13	-0.035
345217.844	60	11	49	60	10	50	-0.004	480643.521	57	10	48	57	9	49	0.012
345853.856	68	14	54	68	13	55	-0.043	480724.826	32	4	28	31	5	27	0.070
346758.212	54	12	42	54	11	43	0.038	480948.882	23	11	13	23	12	12	0.067
349217.705	43	9	35	43	8	36	0.011	481284.899	22	12	10	22	11	11	0.053
350846.409	56	9	47	56	10	46	0.080	481573.367	21	11	11	21	12	10	0.078
350924.669	24	9	15	24	8	16	-0.000	482025.526	19	12	8	19	11	9	0.045
351750.595	24	2	22	23	3	21	-0.009	482197.690	18	12	6	18	11	7	0.090
352049.640	32	2	30	32	3	29	-0.072	482338.944	17	12	6	17	11	7	0.042
352166.952	23	9	15	23	8	16	0.002	482453.000	16	12	4	16	11	5	0.032
352473.257	26	0	26	25	1	25	-0.022	482543.227	15	12	4	15	11	5	0.069
352635.552	61	15	47	60	16	44	0.035	482612.637	14	11	3	14	12	2	0.020
352678.296	25	2	24	24	1	23	0.003	482664.276	13	11	3	13	12	2	-0.006
353125.696	22	9	13	22	8	14	-0.026	482700.829	12	11	1	12	12	0	-0.054
353134.340	24	3	21	23	4	20	-0.006	483026.282	58	8	50	58	9	49	-0.079
353467.849	52	12	40	51	13	39	0.036	484470.052	31	5	27	30	4	26	-0.007
353993.105	37	6	32	37	5	33	-0.023	485175.837	44	4	40	44	3	41	-0.002
354010.425	21	9	13	21	8	14	-0.017	485296.138	35	1	35	36	0	36	-0.029
354728.695	52	9	43	52	8	44	-0.008	485319.003	11	8	4	10	7	3	0.008

Table 1. Continued

Measured frequency f_m	Lower level			Upper level			Residual $f_m - f_c$	Measured frequency f_m	Lower level			Upper level			Residual $f_m - f_c$
	J	K_a	K_c	J'	K'_a	K'_c			J	K_a	K_c	J'	K'_a	K'_c	
354740.915	20	8	12	20	9	11	-0.042	485412.846	35	2	34	34	1	33	0.011
355166.630	8	6	2	7	5	3	-0.011	485613.870	34	2	32	33	3	31	0.011
355188.665	48	7	41	48	8	40	0.083	489127.237	13	6	8	14	7	7	-0.026
355374.855	30	2	28	30	1	29	0.014	489146.880	16	5	11	17	6	12	-0.013
355376.425	19	9	11	19	8	12	-0.038	492061.297	42	8	34	41	9	33	-0.036
355908.365	18	9	9	18	8	10	-0.019	492456.205	47	13	35	47	12	36	0.011
356088.655	28	1	27	28	0	28	0.019	493318.520	63	14	50	63	13	51	0.074
356357.005	17	8	10	17	9	9	0.002	493374.523	66	11	55	66	10	56	-0.007
356548.110	18	3	15	19	4	16	0.032	493439.116	55	9	47	55	8	48	0.010
356823.575	38	9	29	38	10	28	-0.023	493646.789	47	6	42	47	5	43	0.048
357034.195	15	8	8	15	9	7	0.005	494453.808	46	13	33	46	12	34	0.011
357281.545	14	8	6	14	9	5	0.048	495605.979	18	4	14	17	3	15	-0.055
357632.575	12	8	4	12	9	3	-0.010	496043.385	61	11	51	61	10	52	0.014
437488.346	25	11	15	25	10	16	-0.006	496402.929	9	9	1	8	8	0	-0.035
437854.260	46	12	34	46	11	35	-0.000	496987.969	61	13	49	61	14	48	-0.042
437888.817	43	6	38	43	5	39	-0.005	497598.904	67	13	55	67	14	54	-0.011
438110.743	24	11	13	24	10	14	-0.027	498010.357	45	13	33	45	12	34	-0.022
438654.591	23	11	13	23	10	14	-0.004	498570.863	36	0	36	37	1	37	0.047
438918.342	16	5	11	15	4	12	-0.001	498684.605	35	2	34	36	1	35	0.059
439126.370	22	11	11	22	10	12	-0.021	498893.912	34	2	32	35	3	33	0.072
439166.654	8	8	0	7	7	1	-0.007	499110.635	33	4	30	34	3	31	0.099
439533.245	21	10	12	21	11	11	-0.053	499871.617	50	5	45	50	6	44	-0.016
439881.478	20	10	10	20	11	9	-0.052	500174.138	44	13	31	44	12	32	-0.013
445463.289	32	0	32	33	1	33	-0.021	500680.723	11	7	5	12	8	4	0.065
$^{82}\text{SeO}_2$, ground state															
73619.097	8	0	8	8	1	7	-0.002	353945.525	14	9	5	14	8	6	-0.006
333130.045	40	10	30	40	9	31	0.034	354134.980	19	4	16	18	3	15	0.000
333871.260	30	9	21	30	8	22	0.001	354147.452	13	9	5	13	8	6	-0.005
335275.030	31	9	23	31	8	24	-0.025	354305.309	12	9	3	12	8	4	-0.018
336350.005	41	9	33	41	8	34	0.019	354425.857	11	9	3	11	8	4	-0.004
337010.870	12	4	8	11	3	9	0.009	354479.200	37	6	32	37	5	33	0.002
337165.579	54	12	42	54	11	43	-0.015	354515.213	10	9	1	10	8	2	0.039
338636.020	25	1	25	24	0	24	0.001	354708.598	44	7	37	44	6	38	0.010
338836.937	31	4	28	31	3	29	-0.009	355159.694	30	2	28	30	1	29	-0.009
339698.640	15	4	12	14	3	11	0.005	355669.960	28	1	27	28	0	28	0.009
340057.265	28	9	19	28	8	20	-0.025	460862.304	38	12	26	38	11	27	0.001
340472.295	48	11	37	47	12	36	-0.003	471256.400	35	1	35	34	0	34	0.029
343138.684	27	9	19	27	8	20	0.004	471374.326	34	1	33	33	2	32	0.029
343641.588	41	8	34	41	7	35	0.022	471609.924	32	3	29	31	4	28	-0.003
344351.087	26	9	17	26	8	18	0.007	471615.336	33	3	31	32	2	30	-0.006
345356.553	40	6	34	40	5	35	-0.021	472185.597	30	12	18	30	11	19	0.019
345377.520	34	4	30	34	3	31	0.021	474456.872	27	12	16	27	11	17	0.016

Table 1. Continued

Measured frequency f_m	Lower level			Upper level			Residual $f_m - f_c$	Measured frequency f_m	Lower level			Upper level			Residual $f_m - f_c$
	J	K_a	K_c	J'	K'_a	K'_c			J	K_a	K_c	J'	K'_a	K'_c	
346248.333	25	9	17	25	8	18	-0.003	474491.452	16	6	10	15	5	11	-0.026
347351.918	64	12	52	64	11	53	-0.002	475049.612	26	12	14	26	11	15	-0.031
347358.990	39	6	34	39	7	33	-0.027	480454.227	49	13	37	49	12	38	0.021
347434.713	24	9	15	24	8	16	-0.010	480513.313	32	4	28	31	5	27	0.007
347938.594	17	4	14	16	3	13	0.013	482779.678	31	5	27	30	4	26	-0.005
348063.589	28	5	23	27	6	22	0.010	484511.128	35	1	35	36	0	36	-0.029
348159.630	43	9	35	43	8	36	-0.003	484626.769	34	1	33	35	2	34	-0.037
349691.674	22	9	13	22	8	14	-0.012	484825.821	33	3	31	34	2	32	-0.060
351902.311	26	0	26	25	1	25	-0.022	492995.939	9	9	1	8	8	0	0.034
351996.057	19	9	11	19	8	12	-0.044	494658.776	44	13	31	44	12	32	-0.007
352101.337	25	2	24	24	1	23	-0.007	497409.569	43	13	31	43	12	32	-0.014
352117.105	32	3	29	32	2	30	0.004	497629.197	12	8	4	11	7	5	-0.005
352540.161	18	9	9	18	8	10	0.016	497764.427	36	0	36	37	1	37	-0.009
352933.279	8	6	2	7	5	3	0.007	497877.319	36	1	35	35	2	34	0.055
353379.580	16	9	7	16	8	8	0.016	498082.363	35	3	33	34	2	32	0.041
353479.940	24	3	21	23	4	20	-0.004	499455.375	42	13	29	42	12	30	-0.000
353692.300	15	9	7	15	8	8	0.003								
$^{74}\text{SeO}_2$, ground state															
340767.953	37	9	29	37	8	30	-0.076	342504.180	29	3	27	29	2	28	-0.007
340969.216	25	1	25	24	0	24	-0.013	343085.681	35	9	27	35	8	28	0.118
341032.420	39	9	31	39	8	32	0.004	343103.199	32	9	23	32	8	24	-0.038
341060.833	24	1	23	23	2	22	0.040	344497.003	23	3	21	22	2	20	-0.008
342446.694	12	4	8	11	3	9	-0.005	355816.491	26	4	22	25	5	21	-0.009
$^{76}\text{SeO}_2$, $\nu_2 = 1$															
331229.154	39	8	32	39	7	33	0.006	347183.237	34	4	30	34	3	31	-0.008
334029.175	6	6	0	5	5	1	0.011	352401.578	24	2	22	23	3	21	-0.034
336026.950	13	4	10	12	3	9	0.024	355203.850	26	4	22	25	5	21	0.011
336108.545	9	5	5	8	4	4	-0.027	356011.727	32	3	29	32	2	30	0.020
336563.575	33	5	29	33	4	30	-0.018	472795.680	35	1	35	34	0	34	0.002
339774.540	25	1	25	24	0	24	0.016	499383.895	37	1	37	36	0	36	-0.002
$^{77}\text{SeO}_2$, $\nu_2 = 1$															
330825.111	36	5	31	36	4	32	0.001	347529.195	34	4	30	34	3	31	-0.002
332766.235	6	6	0	5	5	1	0.000	352161.360	24	2	22	23	3	21	-0.000
334930.613	13	4	10	12	3	9	-0.001	498943.667	37	1	37	36	0	36	-0.002
336718.940	33	5	29	33	4	30	0.002	499272.861	36	1	35	35	2	34	0.805
343081.758	12	4	8	11	3	9	0.001								
$^{78}\text{SeO}_2$, $\nu_2 = 1$															
333582.895	42	10	32	42	9	33	0.006	438490.141	13	6	8	12	5	7	0.024
333862.940	13	4	10	12	3	9	0.018	445762.739	32	1	31	31	2	30	0.000
333935.955	26	1	25	26	0	26	0.015	471971.601	35	1	35	34	0	34	-0.038
334018.545	9	5	5	8	4	4	-0.032	472305.150	34	1	33	33	2	32	0.016

Table 1. Continued

Measured frequency f_m	Lower level			Upper level			Residual $f_m - f_c$	Measured frequency f_m	Lower level			Upper level			Residual $f_m - f_c$
	J	K_a	K_c	J'	K'_a	K'_c			J	K_a	K_c	J'	K'_a	K'_c	
336869.540	33	5	29	33	4	30	0.038	472778.744	33	3	31	32	2	30	0.023
339181.235	25	1	25	24	0	24	0.061	472799.194	32	3	29	31	4	28	0.018
339490.500	24	1	23	23	2	22	-0.023	485243.331	35	1	35	36	0	36	-0.070
340489.230	37	9	29	37	8	30	-0.064	490832.551	31	12	20	31	11	21	0.083
342469.105	35	9	27	35	8	28	0.018	493226.886	28	12	16	28	11	17	0.032
342774.431	31	4	28	31	3	29	-0.004	493534.007	35	7	29	36	6	30	-0.043
346223.540	41	9	33	41	8	34	-0.033	493857.025	27	11	17	27	12	16	-0.069
346412.894	29	3	27	29	2	28	-0.020	494414.252	26	12	14	26	11	15	-0.022
346813.798	52	9	43	52	8	44	0.000	494904.645	25	11	15	25	12	14	-0.081
347398.459	15	4	12	14	3	11	0.032	494986.891	11	8	4	10	7	3	0.014
347600.845	27	2	26	27	1	27	-0.014	495334.066	24	12	12	24	11	13	0.029
349411.445	10	5	5	9	4	6	-0.022	495707.599	23	12	12	23	11	13	0.011
351923.603	24	2	22	23	3	21	-0.013	496030.394	22	12	10	22	11	11	0.015
352464.118	26	0	26	25	1	25	-0.011	496494.400	17	6	12	16	5	11	-0.022
352894.158	25	2	24	24	1	23	0.013	496739.998	19	12	8	19	11	9	-0.009
352944.604	48	11	37	48	10	38	-0.001	497146.833	16	11	5	16	12	4	0.019
355309.811	28	9	19	28	8	20	0.018	497527.140	14	7	7	13	6	8	-0.011
355667.938	40	10	30	40	9	31	-0.015	498513.723	37	1	37	36	0	36	0.078
355874.453	43	9	35	43	8	36	0.019	498842.286	36	1	35	35	2	34	0.045
355875.523	17	4	14	16	3	13	-0.026	499652.397	33	4	30	34	3	31	-0.040
357273.973	37	6	32	37	5	33	0.043								
$^{80}\text{SeO}_2, \nu_2 = 1$															
330533.985	35	6	30	35	5	31	0.036	460633.482	31	4	28	30	3	27	-0.050
333279.980	36	5	31	36	4	32	0.005	460999.660	8	7	1	9	8	2	0.015
333538.660	26	1	25	26	0	26	0.017	465784.684	42	11	31	42	12	30	-0.002
337013.175	32	9	23	32	8	24	0.021	471179.156	34	0	34	35	1	35	-0.048
337101.930	37	9	29	37	8	30	0.001	471510.878	34	1	33	33	2	32	-0.005
337158.410	33	5	29	33	4	30	0.041	471976.140	33	3	31	32	2	30	-0.048
338485.150	39	9	31	39	8	32	0.031	472066.606	32	3	29	31	4	28	-0.011
338610.687	25	1	25	24	0	24	-0.001	474026.205	39	12	28	39	11	29	-0.017
338632.690	28	5	23	27	6	22	-0.006	481092.025	35	12	24	35	11	25	-0.010
338924.505	24	1	23	23	2	22	0.007	482462.838	34	11	23	34	12	22	0.104
341029.088	12	4	8	11	3	9	0.003	484428.812	35	1	35	36	0	36	0.005
342093.196	23	3	21	22	2	20	0.009	484758.442	35	2	34	34	1	33	-0.033
342224.173	33	9	25	33	8	26	0.017	484854.562	32	12	20	32	11	21	-0.011
344034.643	41	9	33	41	8	34	0.003	484978.408	46	4	42	46	5	41	0.008
344976.466	40	6	34	40	5	35	0.026	485172.284	34	2	32	33	3	31	-0.024
345047.205	15	4	12	14	3	11	0.020	490492.966	24	12	12	24	11	13	0.020
345569.805	30	9	21	30	8	22	-0.003	490546.167	51	12	40	51	13	39	0.005
346202.841	29	3	27	29	2	28	0.015	490876.575	23	12	12	23	11	13	0.027
346406.869	31	8	24	31	9	23	-0.041	490981.761	44	3	41	44	4	40	-0.032
347176.813	27	2	26	27	1	27	0.003	491208.269	22	11	11	22	12	10	0.091

Table 1. The and

Measured frequency f_m	Lower level			Upper level			Residual $f_m - f_c$	Measured frequency f_m	Lower level			Upper level			Residual $f_m - f_c$
	J	K_a	K_c	J'	K'_a	K'_c			J	K_a	K_c	J'	K'_a	K'_c	
347420.394	10	5	5	9	4	6	-0.030	491492.688	21	12	10	21	11	11	0.014
347816.389	41	8	34	41	7	35	-0.029	492107.455	18	12	6	18	11	7	-0.006
349249.222	40	9	31	40	10	30	0.020	492246.196	17	12	6	17	11	7	-0.048
351871.571	26	0	26	25	1	25	0.005	492358.033	16	12	4	16	11	5	-0.038
352036.746	24	3	21	23	4	20	0.001	492446.225	15	12	4	15	11	5	-0.050
352250.334	44	6	38	44	7	37	-0.017	493422.294	52	6	46	52	7	45	-0.004
352293.648	25	2	24	24	1	23	0.002	493859.641	17	6	12	16	5	11	-0.005
353325.806	17	4	14	16	3	13	0.064	494652.805	13	6	8	14	7	7	-0.021
354208.358	27	9	19	27	8	20	-0.007	494686.028	42	2	40	42	3	39	-0.009
354480.362	43	9	35	43	8	36	-0.063	496492.288	40	1	39	40	2	38	-0.026
355452.735	26	8	18	26	9	17	-0.001	497312.804	49	13	37	49	12	38	-0.067
357238.955	25	8	18	25	9	17	0.043	497398.285	17	3	15	18	4	14	0.012
437822.018	33	11	23	33	10	24	-0.017	497676.865	36	0	36	37	1	37	-0.035
439327.219	32	11	21	32	10	22	-0.053	497904.494	35	7	29	36	6	30	0.029
445621.371	7	7	1	8	8	0	-0.090	498003.811	35	2	34	36	1	35	0.047
445912.085	26	10	16	26	11	15	0.020	498007.646	55	8	48	55	9	47	0.034
447768.387	23	11	13	23	10	14	0.009	498428.723	34	2	32	35	3	33	0.068
449272.912	19	10	10	19	11	9	0.018	498599.243	48	13	35	48	12	36	-0.023
460388.838	26	4	22	27	5	23	0.022	498834.393	33	4	30	34	3	31	0.060
460590.317	54	12	42	54	13	41	0.039	499276.392	47	5	43	47	6	42	-0.008
$^{82}\text{SeO}_2, \nu_2 = 1$															
330900.416	35	6	30	35	5	31	-0.002	352437.507	24	3	21	23	4	20	0.001
335264.065	35	9	27	35	8	28	0.026	354863.296	24	9	15	24	8	16	-0.049
342293.341	7	6	2	6	5	1	-0.000	356284.286	32	3	29	32	2	30	0.002
342703.423	31	9	23	31	8	24	-0.077	497197.033	36	1	35	35	2	34	0.005
347612.910	28	9	19	28	8	20	0.035	497616.237	35	3	33	34	2	32	-0.006
351824.689	26	9	17	26	8	18	0.066								

[27]. Then the usual bootstrap method [37] was employed for further assignment. The rotational and centrifugal distortion constants, as derived from an analysis of Watson's Hamiltonian A -reduced form (in the I^r coordinate representation [38]) are listed in Table 2. For the sake of convenience, the first line of Table 2 presents, next to the species notations, the natural abundances of selenium isotopes. The statistical uncertainties for the parameters are shown as a single standard deviation pertaining to the two last digits given in parentheses. Additionally, the weighted root-mean-square deviations ($wrms$, dimensionless) of the spectra are shown for each isotope species. Note, we have fitted the available data with the $wrms$

close to 1, *i.e.* mostly within the experimental error. The number of assigned transitions, N , and maximum values of the quantum numbers J_{max} and $K_{a\ max}$ are indicated as well.

In contrast to other isotopic species, no previous data were available about the $^{74}\text{SeQ}_2$ molecule because of the very low natural concentration of ^{74}Se (0.87%). In order to perform a search for this species' lines, we used an approach as follows to obtain initial estimates for the rotational and quartic centrifugal distortion constants. Initial values of the constants A , B , and C were estimated through extrapolating the data for the rest of species from Table 2. The dimensionless constants A , B , and C are shown in Fig. 1 in

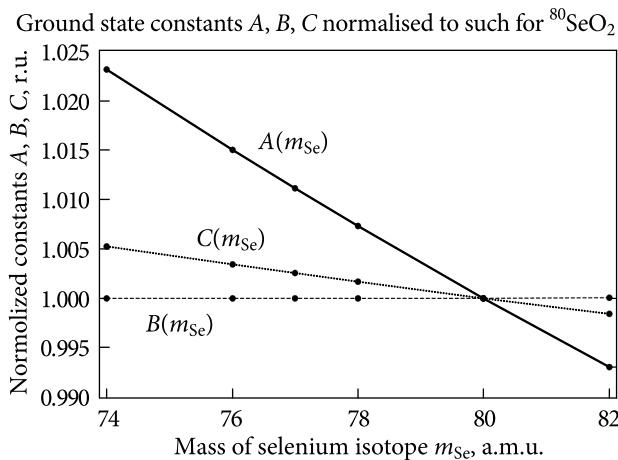


Fig. 1. Values of the A , B , C constants: normalized to such for the $^{80}\text{SeO}_2$ molecule and shown as functions of mass m_{Se} of the selenium isotope in its ground state

dependence on the mass of the selenium isotope m_{Se} (for convenience, all of the constants have been normalized to corresponding values for the $^{80}\text{SeO}_2$ species). It should be noted that the atom of selenium sits directly on the b -axis of the molecule, whence minor changes in the rotational constant B can be observed, following mass variations of the Se isotope (see Fig. 1). A similar approach was used when estimating initial values of the quartic centrifugal distortion constants. An example of the (Δ_K vs mass m_{Se}) dependence for the case of a selenium isotope is shown, as a dashed line, in Fig. 2. The constants obtained in the way just described were used for an initial search of lines. Also, we performed some additional measurements, and finally were able to tentatively assign 10 rotational transitions belonging to

Table 2. Rotational and Centrifugal Distortion Constants (MHz) of Selenium Dioxide in the ground state

Parameter	$^{74}\text{SeO}_2$ (0.87%)	$^{76}\text{SeO}_2$ (9.02%)	$^{77}\text{SeO}_2$ (7.58%)	$^{78}\text{SeO}_2$ (23.52%)	$^{80}\text{SeO}_2$ (49.82%)	$^{82}\text{SeO}_2$ (9.19%)
C	6686.8829(120)	6674.76853(53)	6668.8709(12)	6663.11079(59)	6651.89889(39)	6641.11081(64)
A	29495.1415(370)	29260.4291(20)	29147.5723(27)	29037.9747(21)	28826.5259(13)	28625.3053(25)
B	8676.4364(170)	8676.55430(53)	8676.5886(11)	8676.62243(51)	8676.68507(39)	8676.74378(63)
$\Delta_J \cdot 10^3$	6.1568(130)	6.19177(48)	6.1883(12)	6.18649(54)	6.17648(41)	6.16815(56)
$\Delta_{JK} \cdot 10^2$	-5.91368(490)	-5.93714(41)	-5.90373(43)	-5.87387(30)	-5.81424(21)	-5.75858(46)
$\Delta_K \cdot 10^1$	6.27310(190)	6.19993(28)	6.15222(24)	6.10772(31)	6.02041(14)	5.93791(28)
$\delta_J \cdot 10^3$	2.18255(260)	2.19985(11)	2.20197(27)	2.20403(13)	2.20805(14)	2.21112(17)
$\delta_K \cdot 10^2$	1.15080(370)	1.13391(34)	1.12526(69)	1.11470(39)	1.09883(47)	1.08430(44)
$H_J \cdot 10^8$	—	1.492(15)	1.513(42)	1.600(19)	1.414(27)	1.444(18)
$H_{JK} \cdot 10^8$	—	-6.28(30)	-5.31(70)	—	-1.82(54)	-5.91(37)
$H_{KJ} \cdot 10^6$	—	-4.368(21)	-4.197(29)	-4.560(34)	-4.384(17)	-4.151(26)
$H_K \cdot 10^5$	—	4.258(12)	4.1300(49)	4.272(25)	4.1624(63)	3.997(13)
$h_J \cdot 10^8$	—	0.7468(42)	0.763(12)	0.8122(76)	0.832(11)	0.7664(67)
$h_{JK} \cdot 10^8$	—	-2.00(24)	-2.76(52)	-6.56(31)	-6.51(62)	-3.31(30)
$h_K \cdot 10^6$	—	3.875(46)	3.901(92)	4.383(29)	4.211(58)	3.757(43)
$L_J \cdot 10^{13}$	—	—	—	—	4.05(73)	—
$L_{JK} \cdot 10^{11}$	—	—	—	-2.82(15)	-2.41(25)	—
$L_{JK} \cdot 10^{10}$	—	—	—	2.97(43)	1.788(71)	—
$L_K \cdot 10^9$	—	—	—	-4.57(67)	-3.662(89)	—
$l_J \cdot 10^{13}$	—	—	—	-2.63(21)	-2.94(35)	—
$l_{JK} \cdot 10^{11}$	—	—	—	1.98(12)	1.89(21)	—
$l_{KJ} \cdot 10^{10}$	—	—	—	-3.39(19)	-2.80(28)	—
$l_K \cdot 10^9$	—	-0.350(78)	—	1.52(35)	0.572(49)	-0.356(100)
$wrms$	1.39	0.53	0.75	0.61	0.77	0.47
N	10	70	51	93	162	67
J_{max}	32	68	60	68	70	64
$K_a max$	9	13	17	16	19	13

the ground state of the molecule $^{74}\text{SeO}_2$ (see Table 1). The values of rotational and centrifugal distortion constants, as derived from the analysis for that species, are also listed in Table 2. At present we are able to state the assignments for the $^{74}\text{SeO}_2$ molecule (although just tentatively). Actually, an additional session of measurements is required in order to confirm the above mentioned assignment.

The rotational spectrum of the SeO_2 molecule was investigated through measurements of certain selected lines, hence no continuous spectral records are available. For this reason we calculated the spectra of all assigned species (at frequencies up to 2500 GHz) in order to demonstrate their general view. The calculations were carried out, based on the values of rotational and centrifugal distortion constants which had been obtained from our analysis. The calculated spectrum is shown in Fig. 3, where some line series for specified values of the quantum number K_a are also indicated. Naturally, the lines of the most abundant isotopic species $^{80}\text{SeO}_2$ are dominant in the simulated spectrum. In Fig. 3, the lines corresponding to the rest of the species are, for the most part, almost invisible. First, they are less intense, and next, in the scale of Fig. 3 they sit rather close to the lines of the $^{80}\text{SeO}_2$ species.

2.2. The excited vibrational states $\nu_2 = 1$ and $\nu_2 = 2$

The results obtained in measurements for the first excited state, $\nu_2 = 1$, of the $^{76}\text{SeO}_2$, $^{77}\text{SeO}_2$, $^{78}\text{SeO}_2$, $^{80}\text{SeO}_2$, and $^{82}\text{SeO}_2$ molecules are listed in Table 1, while such for the excited state $\nu_2 = 2$ of $^{80}\text{SeO}_2$ are shown in Table 3. The structure of the two

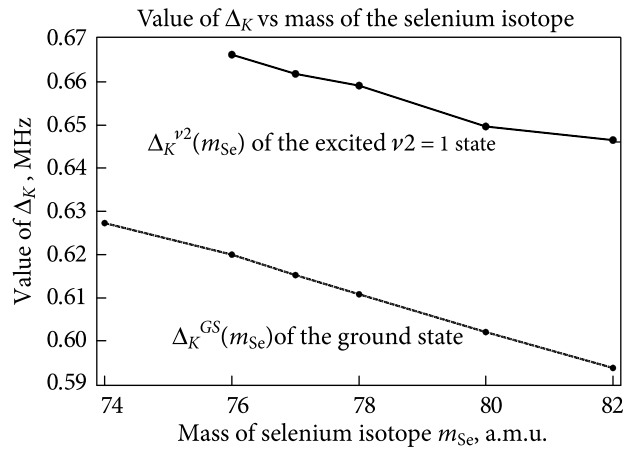


Fig. 2. Values of the Δ_K (MHz) constant in dependence of mass m_{Se} of the selenium isotope in its ground- and first excited ($\nu_2 = 1$) states

Tables is quite similar and it was described above in Section 2.1.

Because of the presence of five quite abundant isotopic species with relatively low-lying excited vibrational states, the experimental spectrum looks as very complicated. Due to the rather high isotope abundances initial assignments for the $^{80}\text{SeO}_2$ (49.82%) and $^{78}\text{SeO}_2$ (23.52%) transitions in the excited state $\nu_2 = 1$, and of $^{80}\text{SeO}_2$ transitions in the excited state $\nu_2 = 2$ were carried out with the use of rotational constants from paper [27] and their corresponding quartic centrifugal distortion constants relating to the ground state.

Note that at the early stage of our investigations the initial assignments for transitions of less abundant species $^{76}\text{SeO}_2$, $^{77}\text{SeO}_2$, and $^{82}\text{SeO}_2$ (all in their excited state $\nu_2 = 1$) were carried out under condi-

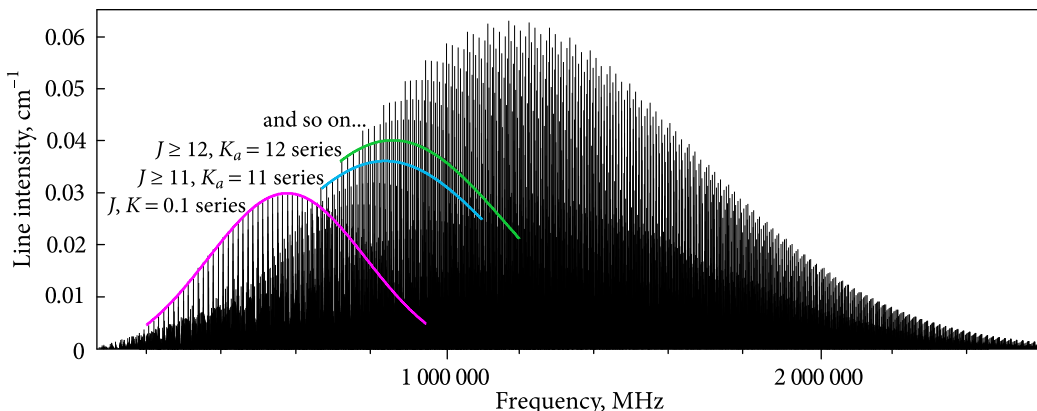


Fig. 3. The calculated spectrum of all investigated SeO_2 species at frequencies below 2500 GHz

Table 3. The excited $\nu_2 = 2$ state transition frequencies (MHz) of $^{80}\text{SeO}_2$ molecule

Measured frequency f_m	Lower level			Upper level			Residual $f_m - f_c$	Measured frequency f_m	Lower level			Upper level			Residual $f_m - f_c$
	J	K_a	K_c	J'	K'_a	K'_c			J	K_a	K_c	J'	K'_a	K'_c	
332856.295	27	6	22	28	5	23	0.014	352880.939	44	6	38	44	7	37	0.001
332868.680	34	8	26	34	9	25	0.020	354152.226	31	9	23	31	8	24	0.004
334077.310	39	7	33	39	8	32	0.004	460614.312	31	4	28	30	3	27	-0.023
334087.060	5	5	1	6	6	0	0.022	470336.102	35	1	35	34	0	34	-0.073
335026.785	12	3	9	13	4	10	0.017	471571.590	33	3	31	32	2	30	0.010
334135.330	35	6	30	35	5	31	0.023	483559.210	36	0	36	35	1	35	0.073
336011.135	9	5	5	8	4	4	-0.017	484105.441	35	2	34	34	1	33	0.042
336429.575	28	2	26	28	1	27	0.007	485150.552	12	6	6	13	7	7	-0.011
336958.850	42	9	33	42	10	32	0.002	495170.112	32	11	21	32	12	20	0.023
338556.597	24	1	23	23	2	22	0.003	496780.589	37	1	37	36	0	36	-0.009
344261.584	37	8	30	37	9	29	-0.043	497078.270	30	11	19	30	12	18	-0.052
346241.859	35	9	27	35	8	28	0.024	497324.121	36	1	35	35	2	34	-0.048
346673.304	40	5	35	40	6	34	-0.001	497968.556	35	3	33	34	2	32	0.014
352064.702	34	3	31	34	4	30	-0.030	498363.945	11	8	4	10	7	3	-0.010
352124.120	41	7	35	41	8	34	0.001	499242.757	27	11	17	27	12	16	0.027

Table 4. Rotational and centrifugal distortion constants (MHz) of selenium dioxide in the excited $\nu_2 = 1$ and $\nu_2 = 2$ states

Parameter	$^{76}\text{SeO}_2 \nu_2 = 1$	$^{77}\text{SeO}_2 \nu_2 = 1$	$^{78}\text{SeO}_2 \nu_2 = 1$	$^{80}\text{SeO}_2 \nu_2 = 1$	$^{82}\text{SeO}_2 \nu_2 = 1$	$^{80}\text{SeO}_2 \nu_2 = 2$
C	6661.3951(42)	6655.5016(27)	6649.7371(25)	6638.5467(14)	6627.7134(42)	6625.1395(33)
A	29703.959(11)	29589.144(18)	29477.5827(57)	29262.3888(29)	29059.388(11)	29712.7078(65)
B	8677.3318(44)	8677.3492(28)	8677.3579(28)	8677.3773(12)	8677.5817(41)	8677.8763(43)
$\Delta_J \cdot 10^3$	6.2114(53)	6.1870(15)	6.1984(30)	6.1877(16)	6.2249(13)	6.19976(424)
$\Delta_{JK} \cdot 10^2$	-6.06923(95)	-6.0184(34)	-6.05165(71)	-5.98831(24)	-5.84769(94)	-6.1744(12)
$\Delta_K \cdot 10^1$	6.6633(20)	6.6173(27)	6.59139(78)	6.49625(37)	6.4648(11)	7.0157(10)
$\delta_J \cdot 10^3$	2.19795(55)	2.20162(49)	2.21085(41)	2.21417(13)	2.2542(14)	2.22024(113)
$\delta_K \cdot 10^2$	1.3531(11)	1.32169(41)	1.3415(11)	1.32297(51)	1.3852(16)	1.5559(23)
$H_J \cdot 10^8$	0.95(19)	—	1.56(10)	1.465(58)	—	1.488(150)
$H_{JK} \cdot 10^8$	—	—	—	—	—	3.14(112)
$H_{KJ} \cdot 10^6$	—	—	-4.875(29)	-4.7440(99)	—	-5.392(56)
$H_K \cdot 10^5$	—	—	4.837(31)	4.728(13)	—	5.564(45)
$h_J \cdot 10^8$	—	—	0.750(17)	0.7574(42)	—	0.7448(432)
$h_{JK} \cdot 10^8$	—	—	-2.02(73)	-2.45(29)	—	-3.85(140)
$h_K \cdot 10^6$	—	—	4.967(23)	4.8280(69)	—	5.658(145)
wrms	0.71	0.81	0.82	0.75	1.39	0.83
N	12	9	49	80	11	30
J_{max}	39	36	52	55	36	44
$K_a max$	8	6	12	13	9	12

tions of a severe lack of experimental data (actually, we only had at our disposal a limited amount of data measured within the 330...360 GHz frequency range). Within that range, lines with relatively high values of the quantum number J were observed. For this reason the number of available transitions was rather limited and corresponded to a quite complicated experimental spectrum. Accordingly, the process of line assignment for the species in the excited state $\nu_2 = 1$ was not straightforward. In order to simplify the procedure it proved necessary to employ the quartic centrifugal distortion constants.

As has been found, the dependences shown by the ground-state rotational and the quartic distortion constants upon the mass m_{Se} of the selenium isotope are mostly linear. Shown in Fig. 2 (dashed line) is, by way of example, the dependence of the ground-state quartic centrifugal distortion constant, $\Delta_K^{\text{GS}}(m_{\text{Se}})$, upon the selenium isotope's mass. Next, we assumed that similar dependences could also take place in the excited state $\nu_2 = 1$. Based on that assumption, we have derived the correspondent linear dependences for all of the ground-state quartic constants, namely

$$\begin{aligned}\Delta_J^{\text{GS}}(m_{\text{Se}}) &= a_{\Delta J} + b_{\Delta J} m_{\text{Se}}, \\ \Delta_{JK}^{\text{GS}}(m_{\text{Se}}) &= a_{\Delta JK} + b_{\Delta JK} m_{\text{Se}}, \\ \Delta_K^{\text{GS}}(m_{\text{Se}}) &= a_{\Delta K} + b_{\Delta K} m_{\text{Se}}, \\ \delta_J^{\text{GS}}(m_{\text{Se}}) &= a_{\delta J} + b_{\delta J} m_{\text{Se}}, \\ \delta_K^{\text{GS}}(m_{\text{Se}}) &= a_{\delta K} + b_{\delta K} m_{\text{Se}}.\end{aligned}\quad (1)$$

The parameters a and b here are coefficients of the correspondent linear approximation functions and m_{Se} is the mass of a proper selenium isotope (specifically, $m_{\text{Se}} = 76, 77, 78, 80$, or 82).

In order to estimate the magnitudes of the quartic constants involved, we used to scale the polynomials of Eq. (1) to the ratio of the corresponding constants of the $^{80}\text{SeO}_2$ molecule in its excited and the ground vibrational state, specifically,

$$\Delta_K^{\nu^2}(m_{\text{Se}}) = (a_{\Delta K} + b_{\Delta K} m_{\text{Se}}) (\Delta_{K80}^{\nu^2}) / (\Delta_{K80}^{\text{GS}}), \quad (2)$$

where Δ_{K80}^{GS} denotes the Δ_K constant for the ground state of the $^{80}\text{SeO}_2$ as the most abundant species, characterized by the natural isotope abundance of 49.82%; $\Delta_{K80}^{\nu^2}$ denotes the value of the Δ_K constant for the excited state $\nu_2 = 1$ of the $^{80}\text{SeO}_2$ isotopic species. Note that Eq. (2) is an example of the scaling procedure for the Δ_K constant only. Similar equa-

tions were applied to estimate all the rest of quartic centrifugal distortion constants (*i.e.*, Δ_J , Δ_{JK} , δ_J , and δ_K) in the excited state $\nu_2 = 1$, for all of the required isotopic species of SeO_2 .

Later we were able to obtain the dependence $\Delta_K^{\nu^2}(m_{\text{Se}})$ for the excited state $\nu_2 = 1$ (see the solid line in Fig. 2). Evidently, our initial assumption was true. The graphs of Fig. 2 also suggest that the dependences obtained for the ground state might be simply scaled to yield (as a first approximation) a similar dependence for the excited vibrational state $\nu_2 = 1$.

Upon substituting mass values (m_{Se} of the selenium isotopes ($m_{\text{Se}} = 76, 77$, or 82) to the scaled polynomials of Eq. (2), we obtain estimates for initial values of the quartic centrifugal distortion constants for corresponding isotopic species of selenium dioxide. Thus, the quartic constants and the rotational ones obtained from paper [27] have allowed us providing an initial assignment of a few targeted transitions. Then the usual bootstrap procedure was applied. Later on we performed an additional session of spectral measurements in order to expand the frequency range (up to 500 GHz) for the entire experimental data set that was available. This way it proved possible to additionally assign some number of transitions.

It should be noted that our calculations allowed predicting a blended line at 499 272.861 MHz which may be attributed either to the $^{77}\text{SeO}_2$ isotope in the excited vibrational state $\nu_2 = 1$, or to the $^{78}\text{SeO}_2$ in the same state. Intensities of the both predicted lines are quite comparable, however we could observe only one in our experiments. The line was finally assigned as belonging to the $^{77}\text{SeO}_2$ ($\nu_2 = 1$) species only. Usually, the central frequencies of blended lines are measured with a reduced accuracy, which was taken into account through application of a weighing scheme. The impact of this line on the final fit was reduced by an order of magnitude, compared with the rest of the lines.

The values of the rotational and centrifugal distortion constants (as derived from the transitions assigned) are shown in Table 4. Once again, the statistical uncertainties for the parameters are shown as one standard deviation for the last two (or three) digits given in parentheses. The weighted root-mean-square deviation $wrms$ of the spectra described is shown for each isotopic species. The number N of

the transitions assigned and maximum values of the quantum numbers J_{max} and $K_a\ max$ are presented as well.

Conclusions

The transitions with quantum numbers J up to 70 and K_a up to 19, belonging to the ground, first, and second excited vibrational states of the molecules $^{74}\text{SeO}_2$, $^{76}\text{SeO}_2$, $^{77}\text{SeO}_2$, $^{78}\text{SeO}_2$, $^{80}\text{SeO}_2$, and $^{82}\text{SeO}_2$ have been assigned. Significantly improved sets of the rotational and centrifugal distortion constants,

including octic ones, of A -reduced Watson's Hamiltonian have been obtained in the I' coordinate representation. The data sets obtained provide reliable predictions for further astronomical search of the most abundant isotopic species.

Acknowledgments. Dr. E. Alekseev gratefully acknowledges the financial support granted by *Le Centre National de la Recherche Scientifique* (CNRS, France) and *l'Université de Lille* (France).

The authors express their thanks to Dr. V.V. Ilyushin for helpful discussions.

REFERENCES

1. Messer, J.K., De Lucia, F.C., Helmingher, P., 1984. Submillimeter spectroscopy of the major isotopes of water. *J. Mol. Spectrosc.*, **105**(1), pp. 139–155. DOI: 10.1016/0022-2852(84)90109-7
2. Bernath, P.F., 2002. The spectroscopy of water vapour: Experiment, theory and applications. *Phys. Chem. Chem. Phys.*, **4**(9), pp. 1501–1509. DOI: 10.1039/B200372D
3. Toureille, M., Koroleva, A.O., Mikhailenko, S.N., Pirali, O., Campargue, A., 2022. Water vapor absorption spectroscopy and validation tests of databases in the far-infrared ($50\text{--}720\ \text{cm}^{-1}$). Part 1: Natural water. *J. Quant. Spectrosc. Radiat. Transf.*, **291**, Id. 108326. DOI: 10.1016/j.jqsrt.2022.108326
4. Karlovets, E.V., Mikhailenko, S.N., Koroleva, A.O., Campargue, A., 2024. Water vapor absorption spectroscopy and validation tests of databases in the far-infrared ($50\text{--}720\ \text{cm}^{-1}$). Part 2: H_2^{17}O and HD^{17}O . *J. Quant. Spectrosc. Radiat. Transf.*, **314**, Id. 108829. DOI: 10.1016/j.jqsrt.2023.108829
5. Jørgensen, U.G., Jensen, P., Sørensen, G.O., Aringer, B., 2001. H_2O in stellar atmospheres, *Astron. Astrophys.*, **372**(1), pp. 249–259. DOI: 10.1051/0004-6361:20010285
6. Aringer, B., Kerschbaum, F., Jørgensen, U.G., 2002. H_2O in stellar atmospheres. II. ISO spectra of cool red giants and hydrostatic models. *Astron. Astrophys.*, **395**(3), pp. 915–927. DOI: 10.1051/0004-6361:20021313
7. Sandor, B. J., Clancy, R. T., 2005. Water vapor variations in the Venus mesosphere from microwave spectra. *Icarus.*, **177**(1), pp. 129–143. DOI: 10.1016/j.icarus.2005.03.020
8. Pickett, H.M., Cohen, E.A., Margolis, J.S., 1985. The infrared and microwave spectra of ozone for the (0, 0, 0), (1, 0, 0), and (0, 0, 1) States. *J. Mol. Spectrosc.*, **110**(2), pp. 186–214. DOI: 10.1016/0022-2852(85)90290-5
9. Ivanov, S.V., Panchenko, V.Ya., 1994. Infrared and microwave spectroscopy of ozone: historical aspects. *Phys.-Usp.*, **37**(7), pp. 677–695. DOI: 10.1070/PU1994v03n07ABEH000034
10. Medvedev, I., Winnewisser, M., De Lucia, F. C., Herbst, E., Białkowska-Jaworska, E., Pszczółkowski, L., Kisiel, Z., 2004. The millimeter- and submillimeter-wave spectrum of the *trans-gauche* conformer of diethyl ether. *J. Mol. Spectrosc.*, **41**(2), pp. 333–380. DOI: 10.1016/j.jms.2004.06.011
11. Alekseev, E.A., Dyubko, S.F., Ilyushin, V.V., Podnos, S.V., 1996. The high-precision millimeter-wave spectrum of $^{32}\text{SO}_2$, $^{32}\text{S}^{34}\text{O}_2$ (v_2), and $^{34}\text{S}^{32}\text{O}_2$. *J. Mol. Spectrosc.*, **176**(2), pp. 316–320. DOI: 10.1006/jmsp.1996.0092
12. Lovas, F.J., 1985. Microwave spectra of molecules of astrophysical interest. XXII. Sulfur dioxide (SO_2). *J. Phys. Chem. Ref. Data*, **14**, pp. 395–488. DOI: 10.1063/1.555729
13. Carlotti, M., Dilonardo, G., Fusina, L., Carli, B., Mencarazlia, F., 1984. The submillimeter-wave spectrum and spectroscopic constants of SO_2 in the ground state. *J. Mol. Spectrosc.*, **106**(1), pp. 235–244. DOI: 10.1016/0022-2852(84)90096-1
14. Helminger, P.A., De Lucia, F.C., 1985. The submillimeter wave spectrum of $^{32}\text{S}^{16}\text{O}_2$, $^{32}\text{S}^{16}\text{O}_2(v_2)$, and $^{34}\text{S}^{16}\text{O}_2$. *J. Mol. Spectrosc.*, **111**(1), pp. 66–72. DOI: 10.1016/0022-2852(85)90069-4
15. Lafferty, W.J., Fraser, G.T., Pine, A.S., Flaud, J.-M., Camy-Peyret, C., Dana, V., Mandin, J.-Y., Barbe, A., Plateaux, J.J., Bouazza, S., 1992. The $3v_3$ band of $^{32}\text{S}^{16}\text{O}_2$: Line positions and intensities. *J. Mol. Spectrosc.*, **154**(1), pp. 51–60. DOI: 10.1016/0022-2852(92)90028-M
16. Maki, A.G., Kuritsyn, Yu.A., 1990. High-resolution measurements of the v_2 and $2v_2-v_2$ bands of $^{34}\text{S}^{16}\text{O}_2$. *J. Mol. Spectrosc.*, **144**(1), pp. 242–243. DOI: 10.1016/0022-2852(90)90319-L
17. Belov, S.P., Tretyakov, M.Y., Kozin, I.N., Klisch, E., Winnerwisser, G., Lafferty, W.J., Flaud, J.-M., 1998. High frequency transitions in the rotational spectrum of SO_2 . *J. Mol. Spectrosc.*, **191**(1), pp. 17–27. DOI: 10.1006/jmsp.1998.7576
18. Alderson, L., Wakeford, H.R., Alam, M.K., et al., 2023. Early release science of the exoplanet WASP-39b with JWST NIR-Spec G395H. *Nature*, **614**, pp. 664–669. DOI: 10.1038/s41586-022-05591-3

19. Powell, D., Feinstein, A.D., Lee, E.K.H. et al., 2024. Sulfur dioxide in the mid-infrared transmission spectrum of WASP-39b. *Nature*, **626**, pp. 979–983. DOI: 10.1038/s41586-024-07040-9
20. Safety data sheet: selenium dioxide. Available from: https://www.integraclear.com/msds/S138_26294_101.pdf
21. Gottlieb, C.A., Ball, J., 1973. Interstellar sulfur monoxide. *Astrophys. J.*, **184**, pp. L59–L64. DOI: 10.1086/181288
22. Snyder, L.E., Hollis, J.M., Ulich, B.L., Lovas, F.J., Johnson, D.R., Buhl, D., 1975. Radio detection of interstellar sulfur dioxide. *Astrophys. J.*, **198**, pp. L81–L84. DOI: 10.1086/181817
23. Abundance in the Universe of the elements. Available from: <https://periodictable.com/Properties/A/UniverseAbundance.v.log.html>
24. Suess, H.E., Urey, H.C., 1956. Abundances of the elements. *Rev. Mod. Phys.*, **28**(1), pp. 53–74. DOI: 10.1103/RevModPhys.28.53
25. Anders, E., Ebihara, M., 1982. Solar-system abundances of the elements. *Geochim. Cosmochim. Acta*, **46**(11), pp. 2363–2380. DOI: 10.1016/0016-7037(82)90208-3
26. Kamiński, T., Gottlieb, C.A., Menten, K.M., Patel, N.A. Young, K.H., Brünken, S., Müller, H.S.P., McCarthy, M.C., Winters, J.M., Decin, L., 2013. Pure rotational spectra of TiO and TiO₂ in VY Canis Majoris. *Astron. Astrophys.*, **551**, Id. A113. DOI: 10.1051/0004-6361/201220290
27. Takeo, H., Hirota, E., Morino, Y., 1970. Equilibrium structure and potential function of selenium dioxide by microwave spectroscopy. *J. Mol. Spectrosc.*, **34**(3), pp. 370–382. DOI: 10.1016/0022-2852(70)90020-2
28. Takeo, H., Hirota, E., Morino, Y., 1972. Third-order potential constants and dipole moment of SeO_2 by microwave spectroscopy. *J. Mol. Spectrosc.*, **41**(2), pp. 420–422. DOI: 10.1016/0022-2852(72)90216-0
29. Alekseev, E.A., Baskakov, O.I., Dyubko, S.F., Polevoi, B.I., 1986. Submillimeter rotational spectrum of the ⁸⁰ SeO_2 molecule. *Opt. Spektros.*, **60**(1), pp. 30–32.
30. Alekseev, E.A., Baskakov, O.I., Dyubko, S.F., 1997. Microwave spectrum of selenium dioxide. *Proc. SPIE*, **3090**, pp. 163–166. DOI: 10.1117/12.267756
31. King, G.W., Meatherall, R.C., 1984. Selenium dioxide: Analysis of the 419-nm absorption system. *J. Mol. Spectrosc.*, **106**(1), pp. 196–216. DOI: 10.1016/0022-2852(84)90093-6
32. Crowther, S.A., Brown, J.M., 2004. The 313 nm band system of SeO_2 . Part 1: vibrational structure. *J. Mol. Spectrosc.*, **225**(2), pp. 196–205. DOI: 10.1016/j.jms.2004.03.005
33. Crowther, S.A., Brown, J.M., 2004. The 313 nm band system of SeO_2 . Part 2: rotational structure. *J. Mol. Spectrosc.*, **225**(2), pp. 206–221. DOI: 10.1016/j.jms.2004.03.006
34. Baskakov, O.I., Moskienko, M.V., Dyubko, S.F., 1975. Investigation of the rotation spectra of HCOOH, DCOOH, HCOOD, and DCOOD in the submillimeter range. *J. Appl. Spectrosc.*, **23**(4), pp. 1377–1379. DOI: 10.1007/BF00618090
35. Alekseev, E.A., Motylenko, R.A., Margulès, L., 2012. Millimeter- and submillimeter-wave spectrometers on the basis of direct digital frequency synthesizers. *Radio Phys. Radio Astron.*, **3**(1), pp. 75–88. DOI: 10.1615/RadioPhysicsRadioAstronomy.v3.i1.100.
36. Alekseev, E.A., Ilyushin, V.V., Budnikov, V.V., Pogrebnyak, M.L., Kniazkov, L.B., 2023. Modernization of the Kharkiv microwave spectrometer: Current state. *Radio Phys. Radio Astron.*, **28**(3), pp. 257–270. DOI: 10.15407/rpra28.03.257
37. Kirchhoff, W.H., 1972. On the calculation and interpretation of centrifugal distortion constants: A statistical basis for model testing: The calculation of the force field. *J. Mol. Spectrosc.*, **41**(2), pp. 333–380. DOI: 10.1016/0022-2852(72)90210-X
38. Watson, J.K.G., 1967. Determination of centrifugal distortion coefficients of asymmetric-top molecules. *J. Chem. Phys.*, **46**(5), pp. 1935–1949. DOI: 10.1063/1.1840957

Received 29.01.2025

С.А. Але́ксеев^{1,2}, О.І. Баска́ков³, С.П. Дюбко^{2,3}

¹ Лабораторія Фізики Лазерів, Атомів і Молекул (ФЛАМ)
Лілльський Університет Корп. Р5 - 59655, Вільньов д'Аск, Франція

² Радіоастрономічний інститут НАН України
вул. Мистецтв, 4, м. Харків, 61002, Україна

³ Харківський національний університет імені В.Н. Каразіна
майдан Свободи, 4, м. Харків, 61022, Україна

МІЛІМЕТРОВИЙ І СУБМІЛІМЕТРОВИЙ СПЕКТР ДІОКСИДУ СЕЛЕНУ SeO_2

Предмет і мета роботи. Роботу було спрямовано на дослідження спектра основного та деяких збуджених станів головних ізотопологів молекули діоксиду селену SeO_2 з метою забезпечити надійну основу для подальшого пошуку в міжзоряному середовищі.

Методи та методологія. Метод дослідження засновано на експериментальних вимірюваннях і наступному аналізі мікрохвильового обертального спектра молекули SeO_2 . Вимірювання виконувалися з використанням автомати-

зованого спектрометра міліметрового діапазону в Радіоастрономічному інституті НАН України (Харків, Україна) і субміліметрового спектрометра в Харківському національному університеті імені В.Н. Каразіна (Харків, Україна).

Результати. Вимірювання проводилися в діапазоні частот між 70 і 500 ГГц, де було виміряно частоти близько 650 обертальних переходів. Більшість з них належать до $^{76}\text{SeO}_2$, $^{77}\text{SeO}_2$, $^{78}\text{SeO}_2$, $^{80}\text{SeO}_2$ та $^{82}\text{SeO}_2$ молекул в основному коливальному стані. Решту ліній було ідентифіковано до $^{76}\text{SeO}_2$, $^{77}\text{SeO}_2$, $^{78}\text{SeO}_2$, $^{80}\text{SeO}_2$ та $^{82}\text{SeO}_2$ ізотопічних різновидів у збудженному коливальному стані $\nu_2 = 1$ і до молекули $^{80}\text{SeO}_2$ у збудженному стані $\nu_2 = 2$. Крім того, було виконано попередню ідентифікацію 10 переходів для $^{74}\text{SeO}_2$ ізотопічного різновиду в основному стані.

Висновки. Було ідентифіковано переходи зі значеннями квантових чисел J аж до 70 і K_a аж до 19, що належать до основного, першого та другого збудженого коливального стану молекул $^{74}\text{SeO}_2$, $^{76}\text{SeO}_2$, $^{77}\text{SeO}_2$, $^{78}\text{SeO}_2$, $^{80}\text{SeO}_2$, та $^{82}\text{SeO}_2$. На основі ідентифікованих переходів було отримано значно вдосконалені набори обертальних сталіх і сталих відцентрових спотворень гамільтоніана Уотсона в A -редукції, включно з октичними, в I^r координатному зображені. Отримані набори параметрів забезпечують надійний прогноз для подальшого астрономічного пошуку найпоширеніших ізотопічних різновидів молекули SeO_2 .

Ключові слова: молекула діоксиду селену, міліметровий спектр, асиметрична дзига, ізотопічне заміщення.